SAND2019-1987C

11th U. S. National Combustion Meeting
Organized by the Western States Section of the Combustion Institute
March 24–27, 2019
Pasadena, California

Fuel Blend Ratio Effects on Ignition and Early Stage Soot Formation

Jacob E. Temme[1,], Stephen Busch[2], Vincent D. Coburn[1], Chol-bum M. Kweon[1]*

[1]CCDC Army Research Laboratory, APG, MD 21005,USA
[2]Sandia National Laboratories, Livermore, CA, 94551, USA
[*]Corresponding Author Email: jacob.e.temme.civ@mail.mil

Abstract: This work presents the results of an experimental investigation into the influence of fuel blend composition on auto-ignition and sooting behavior. Fuel blends were constructed by volumetric mixing of a reference jet fuel (F-24) and an alcohol to jet (ATJ) renewable jet fuel in 20% increments. The combustion of each blend was measured in a constant pressure flow-through chamber. Ambient conditions were varied between 825K to 900K and 6 to 9 MPa. Fuel injection quantity and rail pressure were also varied between 5 mg at 110 MPa and 10 mg at 145 MPa. The optical diagnostic Diffuse Backlight Illumination (DBI) was employed at frame rates up to 45 kHz. These measurements showed that increasing ATJ volume concentrations resulted in significant delays in ignition with decreased first stage ignition reactions. However, increasing ATJ concentration also led to dramatic reductions in early stage soot formation and growth.
Keywords: Fuel Blends, Sprays, Ignition, Soot Formation

1. Introduction

Improved operations of internal combustion propulsion systems is of interest to both civilian and military applications. While both communities share an interest in improvements in efficiency and operability, there exist unique challenges for military use. Due to the Department of Defense Single Fuel Forward Policy [1], F-24 jet fuel is used across the department including in compression ignition systems. This results in a range of issues adapting systems primarily designed for diesel fuels to jet fuels. Additionally, existing petroleum based jet fuels exhibit a wide range in fuel properties [2,3]. Increasing the tolerance of engine systems to naturally occurring fuel property variation will increase the reliability and reduced the required logistical footprint of deployed systems.

Additionally, there has been significant recent efforts to develop bio-derived fuels. For civilian applications these fuels can reduce the environmental impact of transportation. For military applications, these fuels can also enable new expeditionary capabilities through fuel generation at forward operating points. While there has been some work on the precise effects of bio-fuel and biofuel blends, for ground applications these have primarily focused on diesel alternatives including from waste grease and rapeseed feed stocks.[4,5,6] There have also been some efforts to quantify alternative jet fuel combustion characteristics. Many of these studies have focused on the chemistry of the ignition process in rapid compression machine and shocktube investigations. [7,8,9] However, in compression ignition systems the physical spray vaporization, time varying ambient thermodynamics, and turbulent flow dynamics all create the initial and boundary conditions for the chemical processes. Therefore, additional insight can be gained through the use

of spray chambers [10,11] Ultimately, a detailed understanding of the effects of bio-derived jet fuels on the ignition and soot formation processes can inform ignition control models and engine control schemes.

2. Methods / Experimental

Experiments were conducted using the High Temperature Pressure Vessel (HTPV) which is a constant pressure flow through style chamber. Greater detail can be found, [11,12] but briefly this chamber enables independent control of ambient temperatures, pressures and oxygen concentrations across regimes relevant to internal combustion systems. As shown in Figure 1, three large windows allow optical access while the fourth side has a modular injector mount. Fuel was injected using a Bosch common rail and a specially modified CRIN3 injector which has a single axial orifice. For the current work, experimental conditions are listed in Table 1. Two injection configurations were measured. The first simulates a medium engine load with 5 mg of fuel injected at 110 MPa. The second simulates a high engine load with 10 mg of fuel injected at 145 MPa.

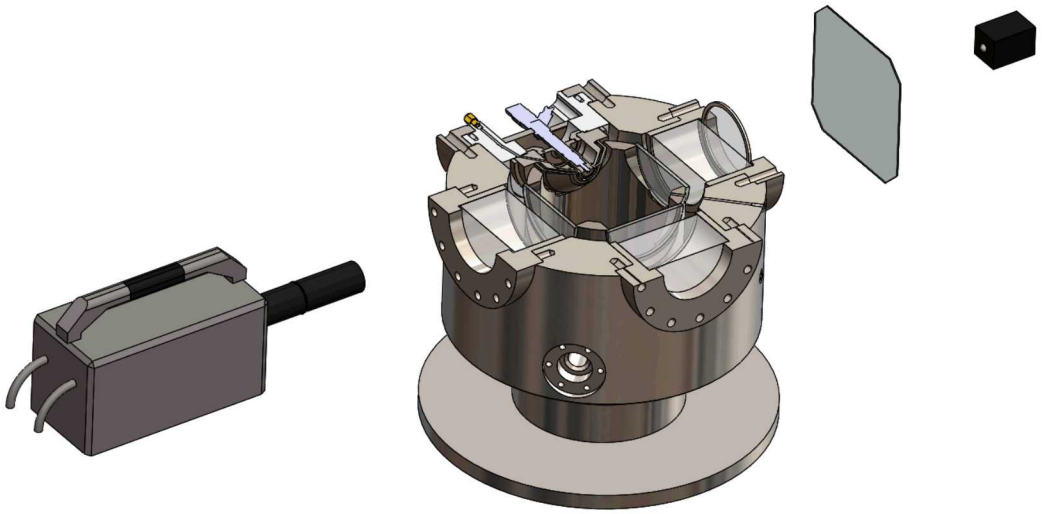

Figure 1: Cutaway view of the High Temperature Pressure Vessel (HTPV). Diffuse Background Illumination optical setup visible to the right consisting of a 405nm LED light source, a Fresnel lens, and an engineered diffuser. Images are recorded by aa SA-X2 camera at the left. On the far side is the modular injector mount.

Experimental Parameter	Units	Range
Chamber Temperature	[K]	825, 900
Chamber Pressure	[MPa]	6, 9
Injection Pressure	[MPa]	110,145
Injection Quantity	[mg]	5,10

Table 1: Experimental parameters

In order to investigate the effects of fuel composition and blend ratio, two fuels were selected. The first is a reference F-24 jet fuel. The second is an alternative jet fuel derived by the alcohol to jet (ATJ) method. Blends were created by mixing volumetrically in 20% increments. Selected fuel properties are shown in Table 2. One of the most critical differences between the two fuels is their cetane number. While ATJ is formulated to meet the specifications of a jet fuel, it has a cetane number of approximately 17, which is similar to a gasoline fuel. Thus, the fuel blend library used in this study exhibits a range of cetane numbers that span both existing variation in jet fuels [2] and potential gasoline fuels. A second important difference to note is the aromatic content, which varies from 15% in the F-24 to less than 1% in the ATJ.

Fuel Property		F24	80F/20A	60F/40A	40F/60A	20F/80A	ATJ
Property	Units						
LHV	[MJ/kg]	43.1	43.4	43.6	43.7	44.0	44.1
Density@15.56□C	[g/cc]	0.804	0.795	0.786	0.777	0.769	0.761
Viscosity@ 40□C	[cSt]	1.377	1.395	1.415	1.446	1.479	1.5
Sulfur	[ppm]	848.4	695.2	543.9	344	187.1	0.4
Cetane Number	[]	48.5	42	35.5	29.4	<21.4	~17
T10	[°C]	176.5	177.1	176.5	177	177.1	178.9
T50	[°C]	207.7	201.2	195.3	189.8	186	183.3
T90	[°C]	250.6	248	245	241	235.5	224.4
Aromatics	[vol%]	15.4	13.1	10	6.3	3.4	0.7
Olefins	[vol%]	1.2	1.2	1	1.4	1.3	1.6
Saturates	[vol%]	83.4	85.6	89	92.4	95.3	97.8

Table 2: Select fuel properties. Fuel blends are noted as volume % F-24/volume % ATJ.

The primary optical diagnostic employed was Diffuse Background Illumination (DBI). This diagnostic combines an LED light source with a structured engineered optic to produce diffuse lighting at the image plane.[13,14,15] It is especially useful to mitigate the large amount of beam steering present in the HTPV. The DBI setup consists of a pulsed 405 nm LED, a Fresnel lens and a 20 degree engineered diffuser from RPC Photonics Inc. Images were recorded utilizing a SA-X2 camera system with a 50mm lens with a filter stack comprised of two 400 +/- 5nm bandpass and two 425nm shortpass filters. The camera was set to record at 90 kHz; however, the LED was alternatively strongly and weakly pulsed every other frame, resulting in image pairs of DBI signal and background natural luminosity at 45 kHz. The resulting field of view is shown in Figure 2 for chamber conditions of 9 MPa and 825K. These conditions normally produce significant beam steering effects visible in other optical setups, i.e schlieren imaging. The region within the dashed circle in 2A shows the effective area within which beam steering effects have been nearly eliminated. This can also be seen as the near constant illumination region in in the centerline cross section plotted in 2B.

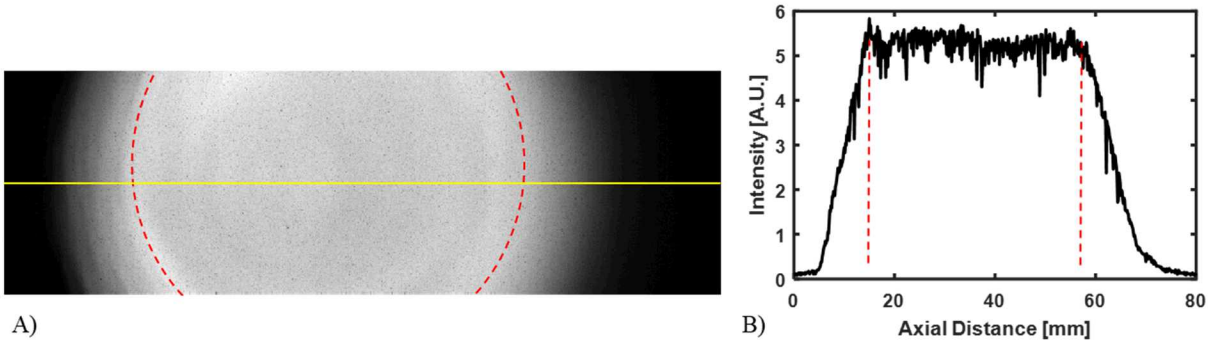

Figure 2: A) the FOV for the DBI setup with 9 MPa and 825K ambient atmosphere. The region inside the red dashed circle is the useful area where the structured optics have nearly eliminated any beam steering effects. B) Instantaneous centerline illumination profile also showing useable region of diffuse lighting at the plane of the injector.

3. Results and Discussion

Example instantaneous raw DBI-extinction images are shown in Figure 3. In 3a) and 3b) the medium and high load injection cases are shown for 825K and 6 MPa. In both cases, fuel blends of 60% and higher ATJ do not exhibit soot formation. However, 60% ATJ does show ignition which can be seen in the edge of the illumination window of the last frame, but no soot growth within the observation window. Additionally, the higher load case shows soot formation sites are more closely concentrated near the centerline axis of the vapor cloud. Increasing the ambient conditions to 900K and 9Mpa, as shown in 3c) and 3d), results in increased soot formation even with fuel blend ratios as high as 80% ATJ.

Figure 4 shows more detailed instantaneous images of the ignition process for two fuels. The images are presented with an inverted false color scheme for visual clarity. In the topmost frame, one can observe the formation of low levels of absorption prior to the radial expansion commonly associated with second stage igition. These time points occur at similar scales to the "disappearing" first stage chemistry seen in schlieren imaging [16]. The signal generated for pure F-24 is higher than for the blended fuels. In the second frame, one can faintly observe the second stage ignition which consumes the absorbant species. Finally in the bottom frame, soot begins to form creating strong extinction signals. For the blended fuel, the ignition event occurs primarily at the leading edge of the vapor cloud in the second frame and only begins to generate soot as it nearly leaves the edge of the FOV. Interestingly, the early stage species formation seems to continue in a spatially layer behind the leading edge resulting in striated combustion zones. At this time, the exact intermediate species absorbing the 405nm light has not been identified. It was confirmed that this early extinction signal was not present when a red 630 nm light was used in place of the 405nm source. It may be generated from the aromatics present in higher amounts in the F-24 fuel. However, it may also be inter-related to the differences in ignition location seen in the high ATJ blends.

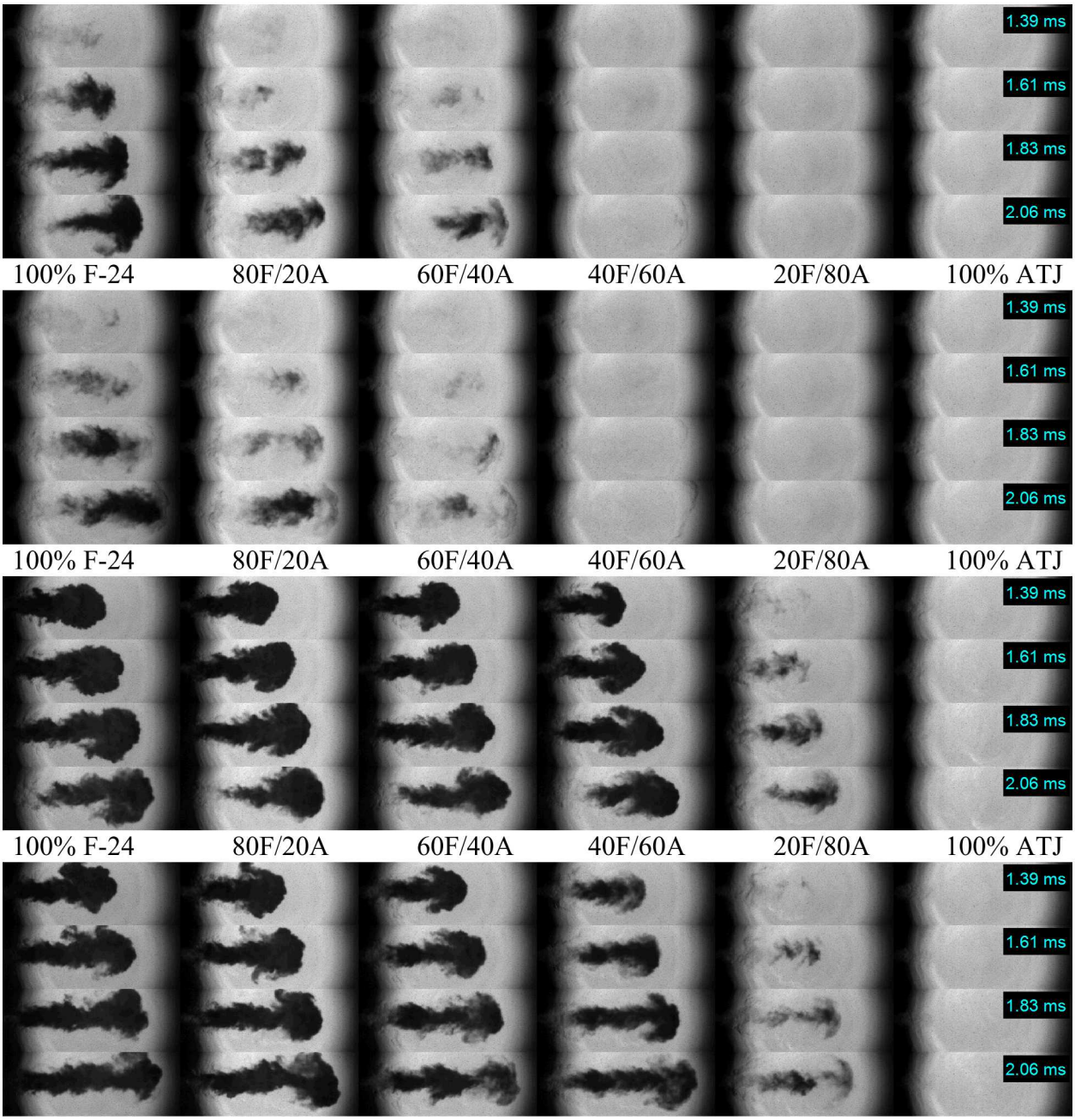

Figure 3a: Images of the raw signal for all blends at 3a) medium load injection and 3b) high load into 825K, 6MPa ambient. Injections of 3c) medium and 3d) high load into 900K and 9MPa show the expected increase in soot formation. Additionally, soot formation is seen in higher ATJ blend ratios.

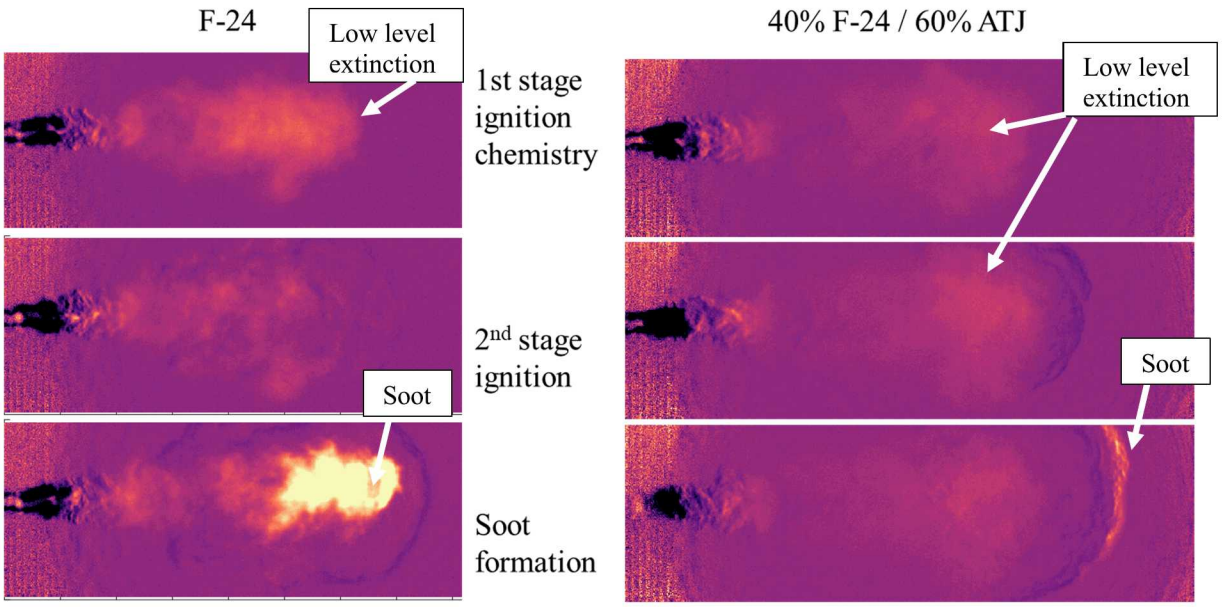

Figure 4: Inverted Raw DBI images for F-24 and Fuel Blend injection of 10mg fuel at 145 MPa into ambient at 825 K, 6 MPa. The F-24 fuel shows low signal levels of absorption during first stage chemistry in the top row. In the middle row, these molecules are consumed during second stage ignition and signal falls. Finally, as seen in the third row, strong absorption by soot molecules is recorded. For the fuel blend, there is much lower amounts of first stage chemistry. Additionally, the second stage ignition only occurs near the leading edge of the vapor cloud. Similarly, soot formation only occurs in a limited region near the vapor leading edge.

These raw images can be converted into KL values by using Eq 1, where α is a negative image calibration factor specific to the camera system. I is the signal intensity and I_{NL} is the natural luminosity at the corresponding pixel of the image pair under the weak LED pulse. Similarly, I_0 and I_{0NL} are the background signals for the respective image pairs.

$$KL = - \log ((1+\alpha) * (I-I_{NL})/ (I_0-I_{0NL})) \quad (1)$$

Example KL fields are shown in Figure 5 for the high load injection into 900K and 9MPa. In these images taken at 1ms post injection, the KL values span from approximately 0.5 to 2. Increasing ATJ blend percentage led to reductions in both magnitude and area of the KL field. Additionally, the pure ATJ still exhibited very little to no measureable soot at these conditions due to its very long ignition delays. However, even small blend amounts of F-24, e.g. 20%, resulted in improved ignition and onset of sooting behavior.

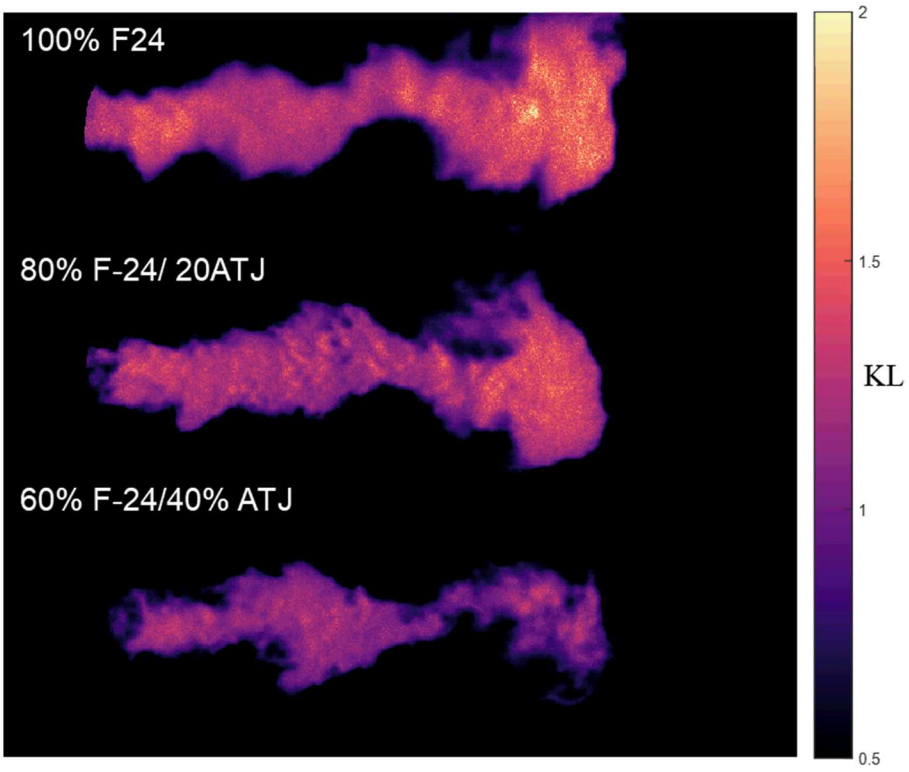

Figure 5: Instantaneous KL fields at 1 ms post injection. Ambient conditions are 900 K and 9 MPa, Injection Pressure is 145 MPa and Injection Quantity of 10 mg. Increasing the ATJ content resulted in lower measured KL. Blend ratios of 40% F-24 and lower did not exhibit measurable KL at this time step.

Figure 6 shows the time history of the frame integrated KL values for each fuel blend at each ambient condition studied under the medium load injection settings. In both 825K cases the initial 1st stage chemistry absorption is seen as an independent rise followed by a secondary soot generation. Increasing temperature from 825 to 900K shows the expected earlier onset of soot due to shorter ignition delays. The increase in temperature results in decreasing the differences between fuel blends. These effects are most pronounced at the highest ambient conditions. Figure 7 shows similar trends at the high load injection settings. First stage ignition is more pronounced at the lowest ambient condition than for the medium load case, likely due to the increased mass of injected fuel. Increasing ambient conditions reduces the effect of fuel blend ratio and property variations; however, there is still a wider variation for the high load cases than the medium load.

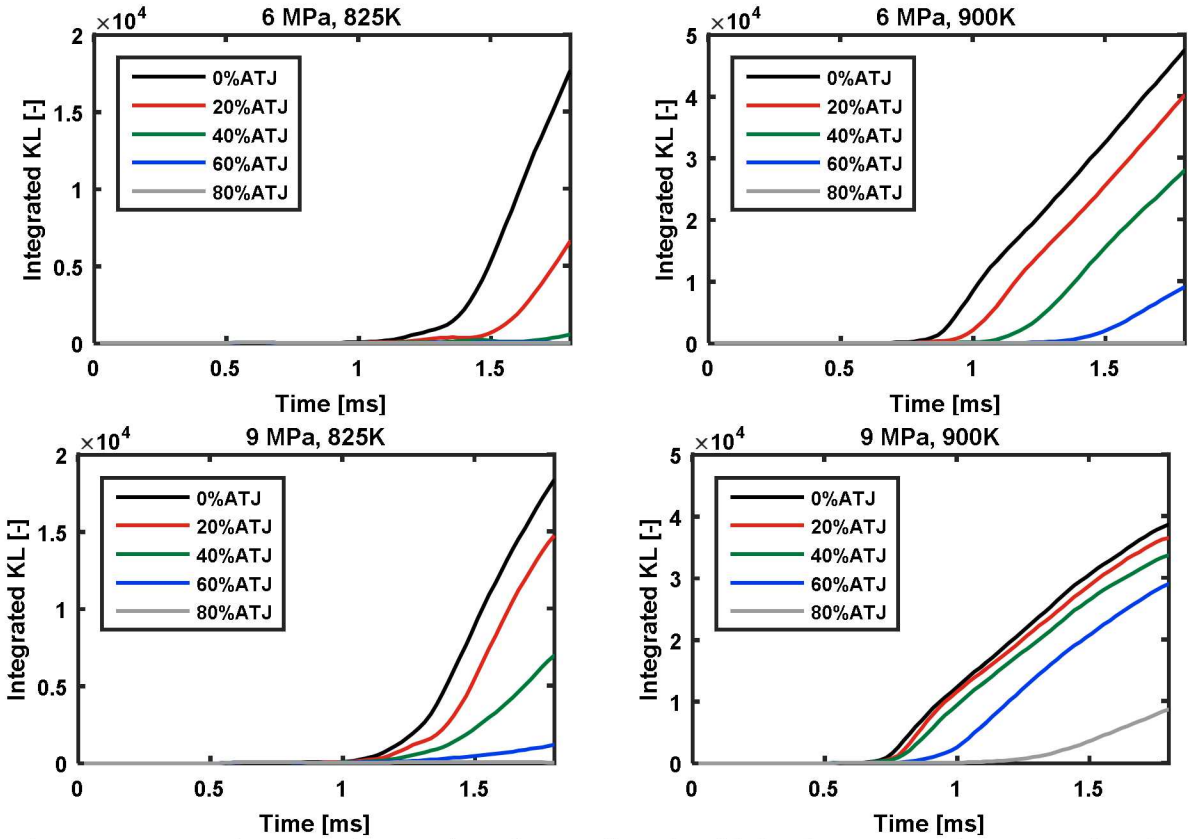

Figure 6: Frame integrated KL values for Medium load injection cases. First stage chemistry is evident at low ambient conditions and tails off as either pressure or temperature increases. Increasing ambient conditions reduces the effect of fuel blend ratio and property variations.

Figure 8 shows the total KL values integrated over an injection event. These values are averaged over twenty injection repetitions. In general, increases in either ambient temperature or pressure result in the expected increase in total KL, with pressure producing the larger effect. There are some discrepancies at for pure F-24 at the higher temperatures; however, these results are likely due to only capturing the initial soot formation period within a specific FOV. For the 6 MPa case, increasing fuel blend percentage of the ATJ leads to an exponential decay of the total KL formation. However, increasing to 9 MPa results in KL formation being mostly constant until blend ratios rise above 60%.

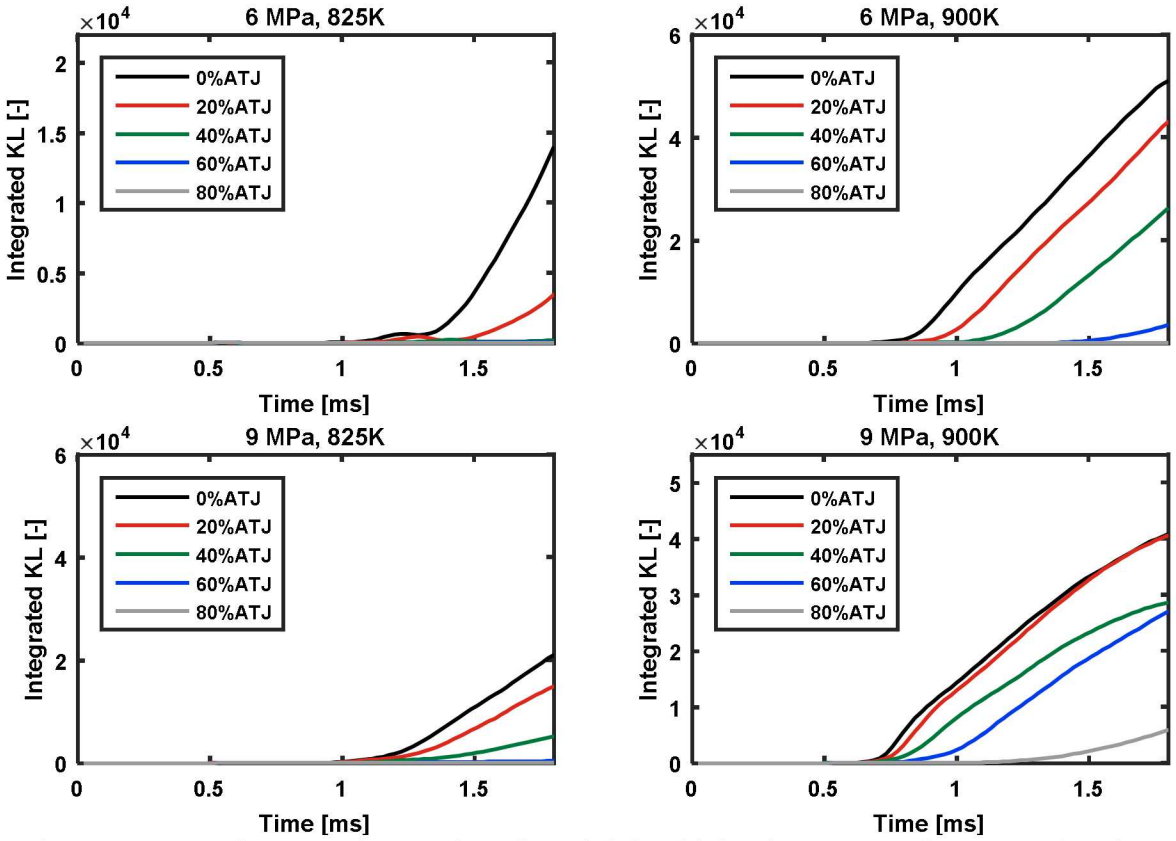

Figure 7: Frame integrated KL values for High load injection cases. First stage chemistry is evident at low ambient conditions. Increasing ambient conditions reduces the effect of fuel blend ratio and property variations; however, there is still a wider variation for the high load cases than the medium load.

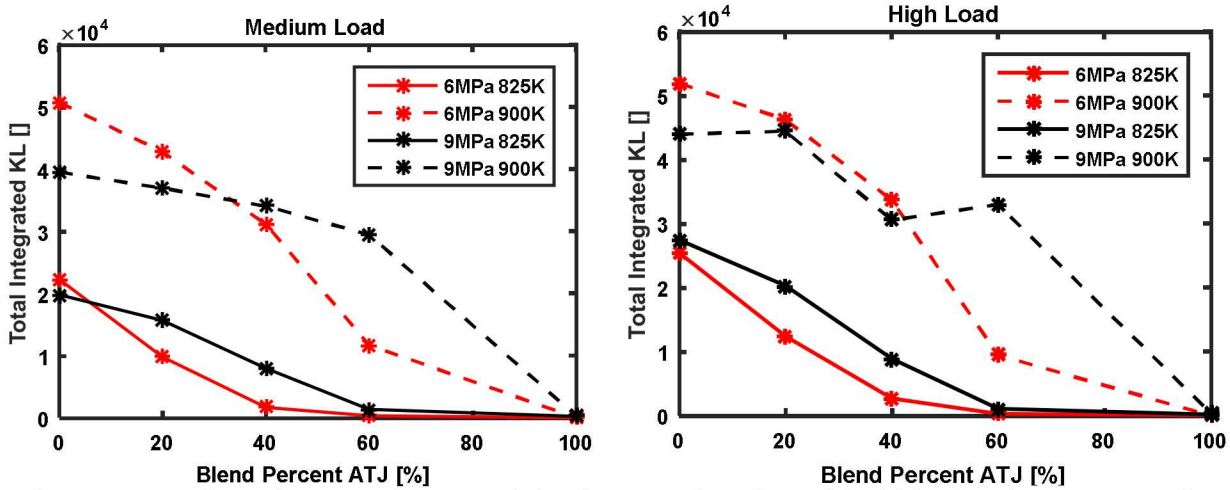

Figure 8: Total KL integrated over an injection as a function of fuel blend ratio. Increases in temperature and pressure generally result in the expected rise in total KL. For the 6MPa cases, increasing ATJ blend % results in decaying total KL. However at 9 MPa, total soot is only slightly affected until ATJ blend % rises above 60%.

4. Conclusions

DBI diagnostics were applied to gain insight into the effects of fuel blend ratios on the ignition and early soot formation process. The effects of ambient conditions were identified for two specific fuel injection settings which simulate a medium and high engine loading. The following conclusions can be made:

- First stage chemistry can be observed due to absorption of some intermediate species as shown particularly clearly at the lower ambient conditions. The precise intermediate species is not known, but does not appear to form in pure ATJ ignition pathways.
- The large ignition delays exhibited by pure ATJ seen here and in [11], may be influenced by the absence of the first stage chemistry that is observed in this study.
- Increasing ATJ leads to decreases in soot formation. This is due in part to the large liftoff and ignition delay leading to excessively lean combustion.
- Increasing ambient conditions lead to the expected increases in soot formation but reduces the differences between fuel blends.
- At 6 MPa conditions, increases in fuel blend concentration lead to exponential decays in total soot formation quantities. However, at 9 MPa the effects increasing fuel blend concentration are relatively modest until blends greater than 60% ATJ.

5. References

1. US Department of Defense, Directive 4140.25, DOD Management Policy for Energy Commodities and Related Services, Section 4.2: Fuel Standardization, Washington, D.C, 2004
2. Petroleum Quality Information System 2013 Annual Report, Defense Logistics Agency Energy, Fort Belvoir, VA.
3. Hadaller, O. J.,Johnson, J. M., "World Fuel Sampling Program," CRC Final Report No. 647, prepared for Coordinating Research Council, Inc., Alpharetta, GA, 2006.
4. Bejaoui S., Lemaire R., Therssen E. "Analysis of Laser-Induced Fluorescence Spectra Obtained in Spray Flames of Diesel and Rapeseed Methyl Ester Using the Multiple-Excitation Wavelength Laser-Induced Incandescence Technique with IR, UV, and Visible Excitations", Combustion Science and Technology, 187:6, (2015) 906-924
5. Desantes, J.M, Payri, R., Garcia, A., Manin, J. "Experimental Study of Biodiesel Blends' Effects on Diesel Injection Processes." Energy and Fuels, 23,6, (2009) 3227-3235
6. Jing, W., Zengyang,W, Roberts, W., Fang, T. "Spray combustion of biomass-based renewable diesel fuel using multiple injection strategy in a constant volume combustion chamber." Fuel, 181,1, (2016) 718-728
7. Hui, X., Kumar, K., Sung, C.J., Edwards, T., Gardner, D. "Experimental studies on the combustion characteristics of alternative jet fuels." Fuel, 98 (2012) 176-182
8. Zhu, Y., Lie, S., Davidson, D.F, Hanson, R.K. "Ignition delay times of conventional and alternative fuels behind reflected shock waves" *Proceedings of the Combustion Institute*, 35, 1, (2015), 241–248
9. Valco, D., et al. "Autoignition behavior of synthetic alternative jet fuels: An examination of chemical composition effects on ignition delays at low to intermediate temperatures" Proceedings of the Combustion Institute, 35,3 (2015) 2983-2991
10. Kook, S., Pickett, L. M. "Liquid length and vapor penetration of conventional, Fischer–Tropsch, coal-derived, and surrogate fuel sprays at high-temperature and high-pressure ambient conditions." *Fuel,* 93, 2012, pp. 539–548
11. Temme, J., Tess, M., Kweon, C.M., Coburn, V. "Alternative Jet Fuel Spray and Combustion at Intermittent-Combustion Engine Conditions" 52nd AIAA/SAE/ASEE Joint Propulsion Conference (2016) AIAA 2016-4689
12. Tess, M., Kurman, M., and Kweon, C., "Spray Characterization and Ignition Delay Measurements of JP-8 and IPK in a Constant-Pressure Flow Chamber," *SAE Int. J. Engines* 9(2) (2016) 899-909
13. Westlye,F.R, Penney, K., Ivarsson, A., Pickett, L., Manin, J., Skeen, S. "Diffuse back-illumination setup for high temporally resolved extinction imaging" Applied Optics, 56,17,(2017) 5028-5038
14. S. A. Skeen, J. Manin, K. Dalen, and L. M. Pickett, "Extinction-based imaging of soot processes over a range of diesel operating conditions" 8th U.S. National Combustion Meeting (2013) 070IC-0355
15. Pastor, J., Garcia-Oliver, J., Novella, R., and Xuan, T., "Soot Quantification of Single-Hole Diesel Sprays by Means of Extinction Imaging," *SAE Int. J. Engines* 8,5 (2015) 2068-2077
16. Benajes, J., Payri, R., Bardi, M., Marti-Aldaravi, P. "Experimental characterization of diesel ignition and lift-off length using a single-hole ECN injector." Applied Thermal Engineering, 58,1-2, (2013) 554-563